Engineering and Technology Journal
Journal homepage: engtechjournal.org

Vision Improvement Using Titanium Dioxide Nanoparticles-Doped PMMA for Contact Lenses

Lina M. Shaker[a]*, Ali H. Al-Hamdani [b], Ahmed A. Al-Amiery[c]

[a] Laser and Optoelectronics Engineering Department, University of Technology-Iraq.
linamohmmed91@gmail.com

[b] Laser and Optoelectronics Engineering Department, University of Technology-Iraq.

[c] University of Technology-Iraq.

*Corresponding author.

Submitted: 27/05/2019 Accepted: 10/10/2019 Published: 25/05/2020

K E Y W O R D S

Contact lens, image simulation, modulation transfer function, nanomaterial, TiO_2-PMMA.

A B S T R A C T

Polymer-based nanocomposites exhibit various optical virtues such as a high refractive index (RI), the dispersion index (Abbe number (v_d)) and visible light transmittance (T %) about 95-99%. Titanium dioxide nanoparticles (TiO_2 NPs) is suggested as a good candidate to rise the RI and maintain high transparency when it is integrated with Poly(methyl methacrylate) polymer PMMA because TiO_2 NPs have a high RI (2.45 and 2.7 for anatase and rutile phase, respectively). The ocular performance was evaluated by modulation transfer function (MTF) and image simulation. The used criteria show that the best visual performance is obtained when TiO_2-PMMA-CL of 0.1 wt/volume of TiO_2 NPs is used ($P < 0.0001$) which reduced the generated spherical and chromatic aberrations inside the eye.

How to cite this article L. M. Shaker, A. H. Al-Hamdani, A. A. Al-Amiery, "vision improvement using titanium dioxide nanoparticles-doped PMMA for contact lenses," *Engineering and Technology Journal*, Vol. 38, No. 05, pp. 681-689, 2020.
DOI: https://doi.org/10.30684/etj.v38i5A.327

1. Introduction

Organic-inorganic hybrid nanocomposites have significantly attracted the attention of researchers and manufacturers due to their high refractive index (RI), the dispersion index (Abbe number (v_d)) and high visible light transmittance [1,2]. Hybrid materials are generally flexible, easy to process, lightweight, gas permeability, mechanically stable, inexpensive and economically viable [3,4]. Therefore, hybrid materials have been employed in contact lenses (CLs) manufacturing.
Fundamentally, CLs classified into hard, soft and rigid gas permeable (RGP) based on their elasticity. Even though hard CLs are longer lasting than the others, but these lenses tend to lose their popularity. Hard CLs are primarily based on hydrophobic materials such as poly (methyl methacrylate) (PMMA), whereas soft CLs are made of biocompatible hydrogels [5,6]. Typically, silicone-hydrogel

or plastic polymers, in addition to the manufacturing techniques used to produce transparent (T > 95%), lightweight and impact-resistant CLs [7,8]. On the other hand, RGP CLs are expensive and suffer from their lack of hydrophilic monomers, but they are more flexible than PMMA CLs due to integration with low modulus components and high efficiency in reducing generated aberrations [9].
Another investigation of CLs materials is poly(vinyl alcohol) (PVA) CLs [10]. These materials exhibit low O_2 permeability and fixed water content, although they have improved physical and optical properties, with a transparency of 90% to visible light [11]. TiO_2 [12,13], ZnO [14], ZnS [15], ZrO_2 [16], Al_2O_3 [17] NPs dopants so far have been utilized to obtain nanocomposites of high optical quality. These nanocomposites can be exploited in CLs manufacturing.

I. Analysis criteria

1.Modulation Transfer Function (MTF)

The MTF considers the contrast degradation that occurs in sinusoidal patterns of spatial frequency. Or it is the ratio of image contrast to object contrast at all spatial frequencies. The spatial frequency that measures the capabilities of the human visual system was examined. The contrast (modulation) of a sinusoidal pattern is defined as [18]:

$$MTF = \frac{I_{Max} - I_{Min}}{I_{Max} + I_{Min}} \quad (1)$$

I_{max}: the irradiance of the peak of the sinusoid
I_{min}: the irradiance of the trough of the sinusoid
At a certain value of spatial frequency the MTF will be zero, this spatial frequency value is called the cutoff frequency ($v_{cut\ off}$) measured in Cycles/mm in this work and it is given by [19]:

$$v_{cut\ off} = \frac{1}{\lambda(F/\#)} \quad (2)$$

F/#: F/number of an optical system refers to the ratio of lens focal length (F) to the pupil diameter (PD).
This work aims to prepare pure PMMA and TiO_2-PMMA with various TiO_2 NPs content because that PMMA has been widely used in CLs. However, no literature is available on using TiO_2-PMMA nanocomposites in CLs up to our knowledge. Then using ZEMAX optical design program to evaluate and modeling the optics of the prepared CLs in comparison with the aberrated human eye. Modulation Transfer Function (MTF) and image simulation have better assisted us in image analysis.

2. Experimental Method

PMMA polymer was prepared using Free Radical Polymerization (FRP) and TiO_2 NPs were prepared using the sol-gel method [20]. The solution casting method was used to prepare the composites with various concentrations of TiO_2 NPs.

I.PMMA preparation

Materials used for PMMA polymer preparation are methyl methacrylate monomer (MMA) ($C_5H_8O_2$) was obtained from Ruby dent, tetrahydrofuran (THF) (C_4H_8O) as solvent and benzoyl peroxide (BPO) ($C_{14}H_{10}O_4$) as initiator. 10 mg of MMA monomer was added to 0.1 g of BPO initiator and THF was added as a solvent. The mixture is then left in a water bath for 24 hours at a temperature of 80°C under nitrogen gas protection. The polymer solution was purified by ethanol twice and left to dry [21].

II.TiO_2-PMMA preparation

Chloroform was used to dissolve the PMMA polymer. 0.1 g of TiO_2 NPs was dispersed in 10 ml of ethanol and xylene mixture (50:50). Various concentrations of 0.001, 0.05, 0.075 and 0.1 ml of the prepared mixture were added to 10 ml of PMMA polymer to obtain the doped TiO_2-PMMA polymer with 0.0001, 0.005, 0.0075 and 0.01 wt/volume, respectively.

III. Scanning Electron Microscope

(SEM) was performed by SEM 54032-GE02-0002/8038 (MIRA3/Austria). Optical properties of prepared nanocomposites were carried out by UV-Vis transmission spectroscopy UV-1601 PC,

(Shimadzu / Japan). The refractive index was measured by Abbe Refractometer at wavelengths 486.1, 587.6 and 656.3 nm whereas the Abbe number was calculated using Abbe formula:

$$\boldsymbol{v_d} = \frac{(\boldsymbol{n_D - 1})}{(\boldsymbol{n_F - n_C})} \quad (3)$$

ν_d: Abbe number

n_C, n_D and n_F: RI of the polymer at wave-lengths of 656, 589 and 486 nm, respectively.

Table 1: Chemical and structural formulas of prepared PMMA and TiO_2-PMMA optical polymers [22].

Polymer abbreviation	Structure	Chemical formula
PMMA	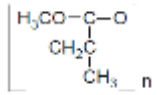	$(C_5O_2H_8)_n$
TiO_2-PMMA	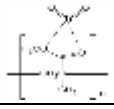	TiO_2-$(C_5O_2H_8)_n$

3. Optical Modeling

ZEMAX optical design program was used for modeling the human eye and the manufactured TiO_2-PMMA CLs. All ray tracing simulations were performed at 5 degree field of view and at the *photopic* spectrum of 470, 510, 555, 610 and 650 nm wavelengths with weights of 0.091, 0.503, 1, 0.503 and 0.107, respectively. Liou and Brennan eye model (LBEM) [23] was chosen for the purpose of evaluating the CLs impact. Input parameters of this model are entered into ZEMAX software as illustrated in Table 2. The anterior and posterior corneal surfaces were selected as aspherical surfaces. the pupil was decentered nasally by 0.5 mm [24,25] and set at 4 mm. The crystalline lens was performed by two homogeneous gradient index shells whose refractive index (n) is described by:

$$n = n_0 + n_{r2}r^2 + n_{r4}r^4 + n_{r6}r^6 + n_{z1}z + n_{z2}z^2 + n_{z3}z^3 \quad (4)$$

$$r^2 = x^2 + y^2 \quad (5)$$

Both of the vitreous body of the eye and the retinal imaging surface was selected as standard surfaces. The standard surface position is centered on the optical axis and its vertex located at the Z-axis. The z-value (sag) of the standard surface is given by [26]:

$$z = \frac{cr^2}{1+\sqrt{1-(1+Kc^2r^2)}} \quad (6)$$

c: curvature (reciprocal of the radius)

r: the radial coordinate in the lens unit

K: conic constant

Construction of the aspherical prepared CLs was done by inserting extended polynomial surface as the front surface of the applied CL. The aspherical surface sag is defined by the expression:

$$z = \frac{cr^2}{1+\sqrt{1-(1+K)c^2r^2}} + \sum_{i=1}^{N} A_i E_i(x,y) \quad (7)$$

N: polynomial coefficients number in the series

A_i: coefficient on the i^{th} extended polynomial (E) term.

The front surface radius of CLs was set at 7.748 mm and it's conic at 0.035 while the back surface was set at 7.8 mm and the prepared CLs thickness has an average of 0.1 mm.

Table 2: Input Parameters Of Liou And Brennan Eye Model In ZEMAX Optical Design [27] Program

Surface	Radius [mm]	Thickness [mm]	RI	ν_d	Conic	PD [mm]
Cornea	7.77	0.55	1.376	50.23	-0.18	10
Aqueous	6.40	3.16	1.336	50.23	-0.6	10
Pupil	Infinity	0	1.34	50.23	0	4
Lens-Front surface	12.40	1.59	-	-	0	10
Lens-Back surface	Infinity	2.43	-	-	0	10
Vitreous humor	-8.1	16.24	1.336	50.23	0.96	10
Retina	-12	-	-	-	0	10

4. Results

A contact lens is prepared by the synthesis of PMMA optical polymer with various TiO_2 NPs concentrations. The synthesized lenses are shown in Figure 1. All of the resulting nanocomposites are transparent, thin and flexible. The thickness of each of the prepared CLs was measured to be 0.1 mm and its diameter of 12 mm.

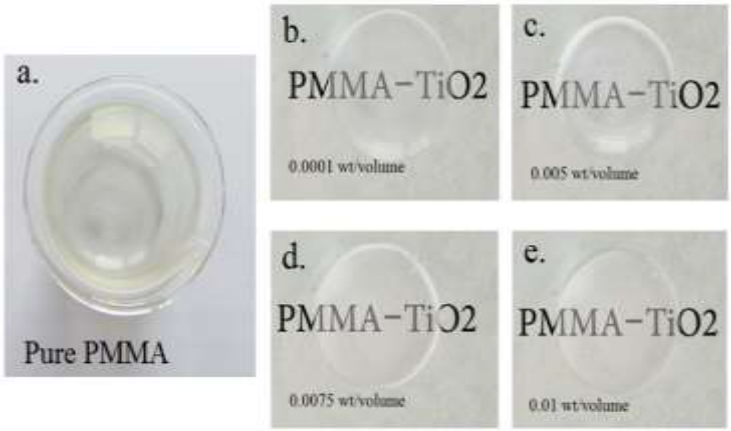

Figure 1: Photographs of prepared samples(a) pure PMMA, (b) TiO_2-$PMMA_{0.0001}$, (c) TiO_2-$PMMA_{0.005}$, (d) TiO_2-$PMMA_{0.0075}$, (e) TiO_2-$PMMA_{0.01}$

I.RI variation with TiO_2 NPs content

RI is an important parameter for CLs. Lens materials with high RI can be cut thinner. This will greatly improve ocular biocompatibility especially for the correction of high myopia. RIs were measured for our CLs from 1.45 to 1.601 as shown in Table 3. RIs of the prepared CLs increased with TiO_2 doping concentration due to the polymer density increment, whereas ν_d shows an opposite trend. Such RIs are superior to human corneas (1.373-1.380) and commercial CLs (1.43) as well as those reported by others [28,29]. As a result of RI variation, the indication of light dispersion namely Abbe number (ν_d) of modified CLs was calculated from Equation 3.

Table 3: Refractive index (RI) and Abbe number (ν_d) data of the prepared CLs

TiO_2 (wt/volume)	RI	ν_d
0	1.45	59.00
0.001	1.495	30.94
0.05	1.497	45.61
0.075	1.503	52.35
0.1	1.602	31.00

II.V-Vis transmission

The UV-vis transmission spectrum shown in Figure 2 indicates that the prepared polymer nanocomposites are highly transparent in the range of 400-700 nm. From the figure, we can observe the difference in light transmittance between pure PMMA about 92% and doped PMMA with TiO_2 NPs about 99%. This is because of the high bandgap of TiO_2 NP which in turn provides these particles excellent optical transmittance. The observed higher transmittance (99%) for prepared TiO_2-PMMA nanocomposites is much better than what has been obtained in earlier researchers investigations (80%) [30,31].

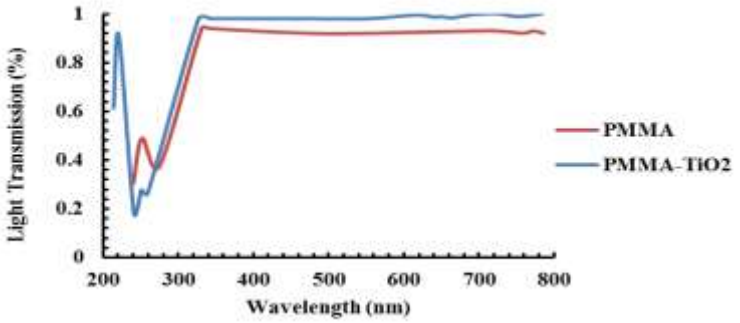

Figure 2: UV-Vis transmittance spectra of the nanocomposite film

III. Morphological Analysis

Scanning electron monographs of prepared TiO_2-PMMA nanocomposites containing 0.001, 0.075, 0.05 and 0.1 wt/volume of TiO_2 NPs are shown in Figures 3-6. From SEM images, it can be seen the TiO_2 NPs as bright points well distributed in the PMMA matrix. This good distribution helps to improve the behavior of the prepared nanocomposites.

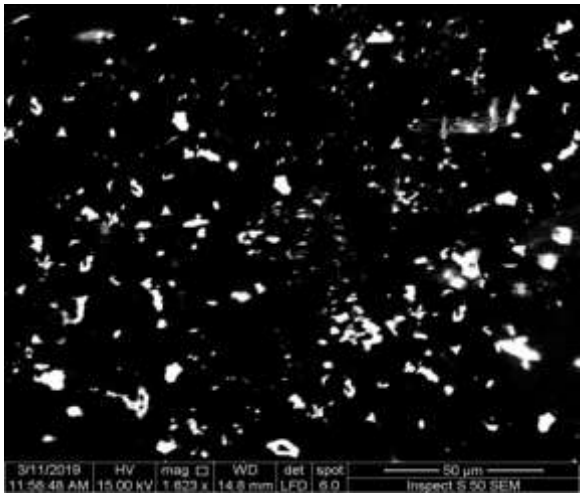

Figure 3: SEM monograph for PMMA-TiO_2 nanocomposite at 0.1 wt/volume of TiO_2 NPs

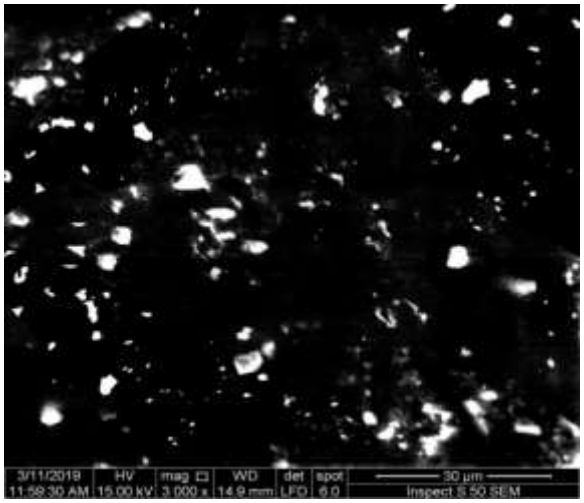

Figure 4: SEM monograph for PMMA-TiO_2 nanocomposite at 0.05 wt/volume of TiO_2 NPs

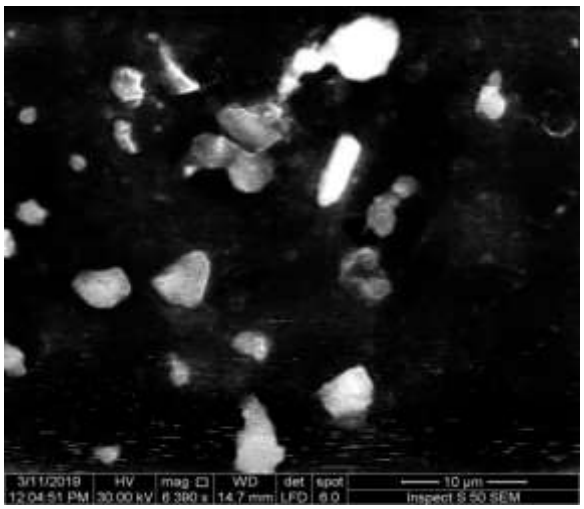

Figure 5: SEM monograph for PMMA-TiO2 nanocomposite at 0.1 wt/volume of TiO2 NPs

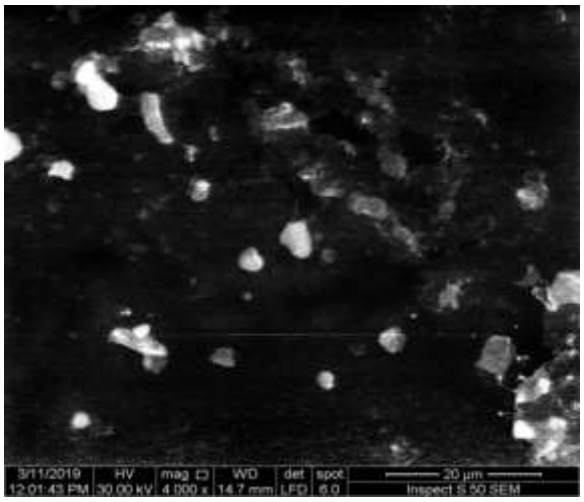

Figure 6: SEM monograph for PMMA-TiO_2 nanocomposite at 0.1 wt/volume of TiO_2 NPs

IV.MTF and image simulation

MTF refers to retinal image contrast as a function of spatial frequency, illustrated in Figure 7. The optimum contrast area achieved by setting the maximum spatial frequency at 30 Cycles/mm. 5-degree off-axis MTF measured at polychromatic light 470-650 nm wavelengths for all models.

The effect of varying TiO_2 concentrations in the PMMA matrix on the characteristics of the retinal image and its comparison with the human eye was studied using the Modulation Transfer Function (MTF). Figure 8 illustrates that high image contrast is achieved at low spatial frequencies, while the contrast of the image at high frequencies prompts how to see the details of a lower image. The highest MTF value is at zero frequency and decreases with increasing frequency.

The best vision is achieved when the area under the curve of the MTF is the largest possible. Therefore, CLs prepared from TiO_2 NPs at a concentration of 0.1 wt/volume illustrate best vision clarity (higher MTF curve, $P < 0.0001$) whereas the other doped CLs exhibit almost similar behavior. The transparency of prepared nanocomposites was lost at concentrations above 0.1 wt/volume. The higher the clarity the better the image properties and the less clarity the less TiO_2 NPs content in the CL. This confirms the impact of RI increase with increased concentration of TiO_2 NPs. The image simulation in Figure 8 reveals the image in Figure 8.f. with 0.1 wt/volume of TiO_2 NPs concentration is more clarity than the image formed by the prepared lens without NPs addition (PMMA-only) as in Figure 8.b. and better than the retinal image formed by the eye without CL as in Figure 8.a.

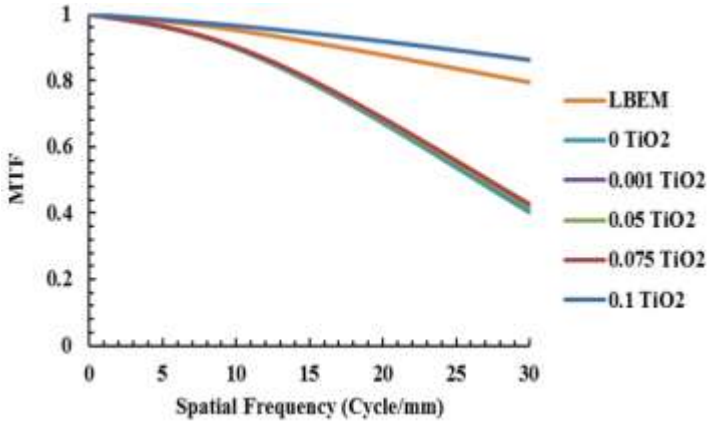

Figure 7: MTF evaluation nm for both aberrated and treated eyes with pure PMMA and TiO_2-PMMA CLs of different TiO_2 content in (wt/volume) at polychromatic light range 470-650

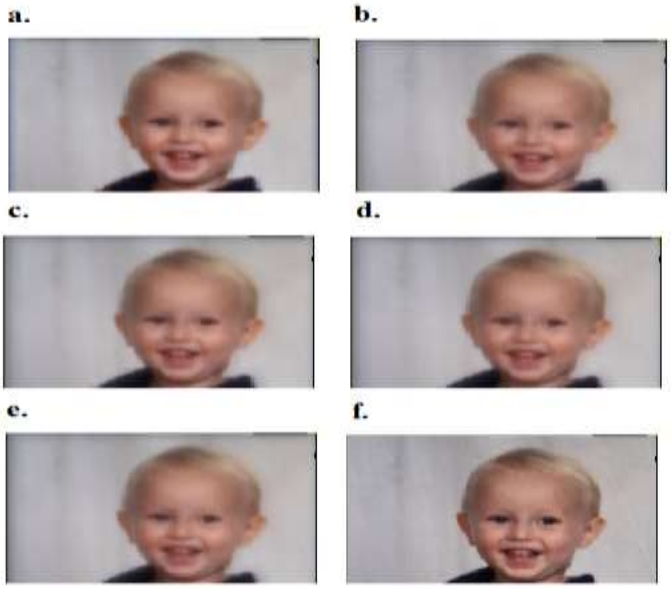

Figure 8: Image simulation at white light (a) LBEM model. (b) undoped CL. (c) 0.001 (wt/volume) TiO_2 doped CL. (d) 0.05 (wt/volume) TiO_2 doped CL. (e) 0.075 (wt/volume) TiO_2 doped CL. (f) 0.1 TiO_2 doped CL

V.X-ray diffraction

The X-ray pattern in Figure (9) shows a notable, highly intense Bragg diffraction peak at 2θ = 19.14°. This intense hump indicates the crystallinity of PMMA polymer. The other diffraction peaks located at 2θ = 25.24°, 43.43° and 67.65° corresponding to (100), (110) and (200) planes of the anatase TiO_2 phase.

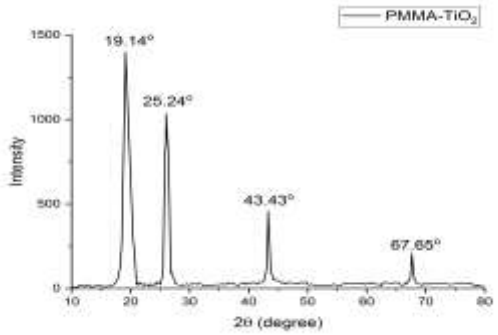

Figure 9: XRD patterns of TiO2–PMMA nanohybrid thin films

4. Conclusion

Transparent nanocomposites of TiO_2 doped PMMA have been prepared by the casting solution method. The impact of doping with various TiO_2 NPs concentrations on structural and optical properties has been studied. From SEM images, TiO_2 NPs appeared well distributed in the polymer matrix. The effect of pure and doped PMMA polymer as a material for CLs manufacturing has been simulated by ZEMAX optical design program. Higher vision clarity in terms of the higher MTF curve was achieved by doping the PMMA with higher TiO_2 NPs concentrations. This is due to the high RI and ν_d along with high transparency in the visible spectral range.

References

[1] F. A. Maulvi, A. A. Shaikh, D. H. Lakdawala, A. R. Desai, M. M. Pandya, S. S. Singhania, R. J. Vaidya, K. M. Ranch, B. A. Vyas, D. O. Shah, "Design and optimization of a novel implantation technology in contact lenses for the treatment of dry eye syndrome: In vitro and in vivo evaluation," *ACTA BIOMATER.*: Vol. 53, pp. 211–221, 2017.

[2] Q. Zhang, Z. Fang, Y. Cao, Du H., H. Wu, R. Beuerman, M. B. Chan-park, H. Duan, R. Xu, "High refractive index inorganic−organic interpenetrating polymer network (IPN) hydrogel nanocomposite toward artificial cornea implants," ACS Macro lett., Vol. 1, pp. 876–881, 2012.

[3] J. -G. Liu and M. Ueda, "High refractive index polymers: Fundamental research and practical applications," *J. Mater. Chem.*, Vol. 19, pp. 8907–8919, 2009.

[4] Y. Chujo and K. Tanaka, "New polymer materials based on element-blocks," *Bull. Chem. Soc. Jpn*, Vol. 88, pp. 633–643, 2015.

[5] F. J. HOLLY, "Basic aspects of contact lens biocompatibility," *Colloids Surf .*, Vol. 10, pp. 343–350, 1984.

[6] T. Goda and K. Ishihara, "Soft contact lens biomaterials from bioinspired phospholipid polymers," *Expert Rev. Med. Devices*, Vol. 3, No. 2, pp. 167–174, 2006.

[7] C. Maldonado-Codina and N. Efron, "Dynamic wettability of pHEMA-based hydrogel contact lenses," *Ophthalmic Physiol. Opt.*, Vol. 26, pp. 408–418, 2006.

[8] E. Seo, S. Kumar, J. Lee, J. Jang, J. H. Park, M.C. Chang, I. Kwon, J. S. Lee, Y. il Huh, "Modified hydrogels based on poly(2-hydroxyethyl methacrylate) (pHEMA) with higher surface wettability and mechanical properties," Macromol. Res, Vol. 25, pp. 704–711, 2017.

[9] F. Shokrollahzadeh, H. Hashemi, E. Jafarzadehpur[c], A. Mirzajani, M. Khabazkhoob[d], A. Yekta, S. Asgari, "Corneal aberration changes after rigid gas permeable contact lens wear in keratokonic patients," *J Curr Ophthalmol.*, Vol. 20, pp. 1–5, 2016.

[10] M. Kita, Y. Ogura, Y. Honda, S.-H. Hyon, W.-I. Cha, Y. Ikada, "Evaluation of polyvinyl alcohol hydrogel as a soft contact lens material," *Graefe's Arch. Clin. Exp. Ophthalmol*, Vol. 228, pp. 533–537, 1990.

[11] G. K. Tummala, R. Rojas, A. Mihranyan, "Poly(vinyl alcohol) Hydrogels Reinforced with Nanocellulose for Ophthalmic Applications: General Characteristics and Optical Properties.," *J. Phys. Chem. B*, Vol. 120, pp. 13094–13101, 2016.

[12] Q. Hao, X. Fu, S. Song, D. Gibson, C. Li, H. Chu, Y. Shi, "Investigation of TiO_2 Thin film deposited by microwave plasma assisted sputtering and its application in 3D glasses," *Coatings*, 8, , Vol. 8, pp. 1–14, 2018.

[13] S. Sathish, B. C. Shekar, B. T. Bhavyasree, "Optimization of bandpass optical filters based on TiO_2 nanolayers," Optical Engineering. *Res.*, Vol. 54, pp. 015101 –7, 2015.

[14] M. M. Demir, K. Koynov, C. Bubeck, I. Park, I. Lieberwirth, G. Wegner, "Optical properties of composites of PMMA and surface-modified zincite nanoparticles," *Macromolecules*, Vol. 40, pp. 1089–1100, 2007.

[15] J. Xu, Y. Zhang, W. Zhu, Y. Cui, "Synthesis of polymeric nanocomposite hydrogels containing the pendant ZnS nanoparticles: approach to higher refractive index optical polymeric nanocomposites," *Macromolecules*, Vol. 51, No. 7, pp. 2672–2681, 2018.

[16] Y. Xia, C. Zhang, J. X. Wang, D. Wang, X. F. Zeng, J. F. Chen, "Synthesis of transparent aqueous ZrO_2 nanodispersion with a controllable crystalline phase without modification for a high-refractive-index nanocomposite film," *Langmuir*, Vol. 34, No. 23, pp. 6806–6813, 2018.

[17] B. Cai, T. Kaino, O. Sugihara, "Sulfonyl-containing polymer and its alumina nanocomposite with high

Abbe number and high refractive index," *Opt. Mater. Express*, Vol. 5, No. 5, p. 1210, 2015.

[18] E. Hecht, "Optics," Pearson education limited, 5th ed., England, p. 579, 2017.

[19] M. Schaub, J. Schwiegerling, E. C. Fest, A. Symmons, R. H. Shepard, "*Molded optics: design and manufacture*," Taylor and Francis Group, LLC, 2011.

[20] F. Kamil, K. A. Hubiter, T. K. Abed, and A. A. Al-Amiery, "Synthesis of aluminum and titanium oxides nanoparticles via sol-gel method : optimization for the minimum size," *J. Nanosci. Technol.*, Vol. 2, No. 1, pp. 37–39, 2016.

[21] M. Stickler, T. Rhein, "Polymethacrylates" in Ullmann's Encyclopedia of Industrial Chemistry, 5th ed., Elvers, B.; Hawkins, S.; Schultz, G. Eds., VHS: New York, 1992, A21, 473.

[22] D. Mauro, A. Cantarella, M. Nicotra, G. Pellegrino, G. Gulino, A. Brundo, M. Privitera, V. Impellizzeri, "Novel synthesis of ZnO/PMMA nanocomposites for photocatalytic applications," Scientific Reports., 2017, Vol., 7, 40895, 2018.

[23] N. A. Brennan and H.-L. Liou, "Anatomically accurate, finite model eye for optical modeling," *Opt. Soc. Am.*, Vol. 14, No. 8, pp. 1684–1695, 1997.

[24] G. Westheimer, "Image quality in the human eye," *Opt. Acta Int. J. Opt.*, Vol. 17, No. 9, pp. 37–41, 1970.

[25] S. Dua, U. R. Acharya, E. Y. K. Ng, "*Computational analysis of the human eye with applications*," World Scientific, 2011.

[26] J. M. Geary, "*Glass, and the land scape lens,"* 2002.

[27] G. Zoulinakis, J. Taboada, T. Blasco, D. Costa, R. Micó. Accommodation in human eye models: a comparison between the optical designs of Navarro, Arizona and Liou-Brennan. Int J Ophthalmol, Vol. 10, pp. 43-50, 2017

[28] Y. Liu, S. Siddiqui, Y. Ji, J. Ge, "Silicone hydrogel contact lenses," U.S patent 9625616 B2, April 18, 2017.

[29] S. Kennedy, J. G. Linhardt, A. Diciccio, "Cast moldable, high RI, rigid, gass permeable polymer formulations for an accommodating contact lens," U.S Patent 0088352 A1, March 29, 2018.

[30] S. Sugumaran and C. S. Bellan, "Transparent nano composite PVA-TiO_2 and PMMA-TiO_2 thin films: Optical and dielectric properties," Optik (Stuttg)., Vol. 125, No. 18, pp. 5128–5133, 2014.

[31] S. Maeda, M. Fujita, N. Idota, K. Matsukawa, Y. Sugahara, "Preparation of transparent bulk TiO_2/PMMA hybrids with improved refractive indices via an in situ polymerization process using TiO_2 nanoparticles bearing PMMA chains grown by surface-initiated atom transfer radical polymerization," ACS Appl. Mater. Interfaces, Vol. 8, No. 50, pp. 34762–34769, 2016.